Hindawi
Shock and Vibration
Volume 2024, Article ID 5582169, 9 pages
https://doi.org/10.1155/2024/5582169

Research Article

HMM-Based Method for Aircraft Environmental Control System Turbofan Rolling Bearing Fault Diagnosis

Gang Yang, Yu Wang, Dezhao Qin, Rui Zhu, and Qingpeng Han

School of Energy and Mechanical Engineering, Shanghai University of Electric Power, Shanghai, China

Correspondence should be addressed to Dezhao Qin; qdzkd@163.com

Received 17 August 2023; Revised 1 February 2024; Accepted 12 February 2024; Published 2 March 2024

Academic Editor: Jinqiang Gan

In response to the high-noise, nonlinear, and nonstationary characteristics of vibration signals from aircraft environmental control system (ECS) turbofan rolling bearings, this paper proposes a diagnostic method for the degree of ECS turbofan bearing faults based on the Hidden Markov Model (HMM). Experimental results demonstrate that HMM can accurately diagnose and predict faults in ECS turbofan rolling bearings. The HMM method enhances diagnostic accuracy, and its effectiveness and feasibility in fault diagnosis based on different rolling bearing fault instances are elaborated. By employing the HMM model to establish precise models from decomposed dynamic data, it successfully identifies faults such as the fracture of the bearing cage under biased load conditions, although its performance in recognizing overheating faults is suboptimal.

1. Introduction

Aircraft environmental control system (ECS) turbofan rolling bearings are susceptible to various typical faults, such as poor lubrication, biased load, excessive dynamic load, high rotational speed, and long-term variable working conditions, which can result in bearing wear, overheating, damage, and skidding [1]. Vibration signals from rolling bearings contain abundant operational state information, and analyzing these signals can provide various characteristic parameters reflecting the fault state of the rolling bearings [2, 3]. The vibration signals of ECS turbofan rolling bearings exhibit time-varying features and periodic impulses under different fault conditions [4]. High-frequency resonance analysis, including envelope analysis, bicoherence analysis, and other frequency domain analysis methods, can identify these characteristics. Time-frequency analysis methods, such as wavelet transform, neural networks, Hidden Markov Model (HMM), and Kalman filtering, have been utilized for analyzing the status of rolling bearing vibration signals [5–8].

In recent years, numerous scholars have utilized various feature representations, including the time-frequency domain, time domain, and frequency domain, for the purpose of diagnosing bearing faults through intelligent methods. Jiang et al. [9] introduced an adaptive detection method that employs variational mode decomposition (VMD) for the early detection of defects in bearings. However, VMD exhibits modal aliasing phenomena, which have a detrimental impact on diagnostic performance [10]. Ning et al. [11] proposed an enhanced intelligent fault diagnosis system for rolling bearings based on ShufflenetV2-LSTM, which significantly improves fault recognition accuracy. Nevertheless, the incorporation of a dropout layer results in model instability and necessitates additional training costs. Mao et al. [12] conducted research on a diagnostic approach that combines optimal feature selection with an adaptive support vector machine (SVM). However, this method is not effective in utilizing all features to differentiate between various fault states.

He and Ma [13] proposed a fault diagnosis methodology leveraging the Fractional Fourier Transform (FRFT) in conjunction with a Deep Belief Network (DBN). This approach is extensively applied to address the intricacies associated with weak faults in rolling bearings, marked by characteristics such as small amplitudes, heightened noise levels, nonlinearity, and inherent instability. The methodology involves the transformation of the original fault signal

into the fractional domain, where subsequent signal filtering facilitates the extraction of distinctive fault features. Following this, the feature signal is fed into the DBN, with the entire network undergoing optimization through pretraining and backpropagation algorithms, ultimately culminating in a precise fault diagnosis. However, challenges emerge when the model encounters scenarios where there is minimal disparity between signals emanating from bearing rolling elements, the cage, and those representing normal data waveforms, particularly in instances where the bearing exhibits subtle faults.

This paper primarily addresses typical fault modes in aircraft environmental control system (ECS) turbofan bearings, such as spalling faults. When the characteristic parameters in the bearing's state evolution exhibit strong nonlinearity rather than following linear patterns, it becomes necessary to perform real-time modeling of historical and current data. This modeling is based on time series models or other control and intelligent models for the purpose of fault prediction.

After an in-depth analysis of existing literature, it becomes apparent that the majority of diagnostic approaches exhibit inherent limitations. Taking the noise-injection-enhanced intelligent mechanical fault diagnosis method proposed by Yang et al. [14] as an illustrative example, this method strategically employs noise injection to dynamically adjust parameters, thereby enhancing diagnostic performance across diverse operational conditions. Its primary focus lies in fortifying the detectability of signals, which is particularly advantageous in scenarios necessitating the identification of weak signals. This heightened sensitivity contributes to an improved discernment of subtle faults. However, it is crucial to acknowledge that the influence of different types of noise injection on the system may vary. In certain situations, the introduction of unforeseen interference through noise injection could detrimentally impact diagnostic accuracy.

In contrast, this paper introduces a predictive methodology grounded in the application of the Hidden Markov Model (HMM). Renowned for its attributes encompassing multistate modeling, autonomous learning, probabilistic diagnosis, and real-time capabilities, the HMM model stands out as an intelligent paradigm. Its discerning sensitivity to time-series data, adeptness in capturing state evolution, and applicability to scenarios featuring relatively slow system state changes make it a powerful diagnostic instrument. These distinctive features position the HMM model as a robust tool with the potential to significantly augment the accuracy and efficiency of aircraft bearing fault diagnosis [15–21]. The anticipated application of the HMM model holds promise for elevating the precision and effectiveness of aircraft bearing fault diagnosis.

In this study, a predictive algorithm tailored to detect typical faults in aircraft environmental control system (ECS) turbofan bearings has been developed through the application of the Hidden Markov Model (HMM). The paper provides a methodology for calibrating and adjusting the parameters of the fault prediction model. Furthermore, the HMM model has been effectively applied to validate faults, including the fracture of bearing cages under biased load conditions and overheating faults.

2. HMM Basic Principles

Hidden Markov Models (HMMs) represent a parametric probabilistic model employed to elucidate the statistical attributes of stochastic processes [22].

Using a discrete first-order Hidden Markov Process as an illustrative instance, the constituents of an HMM are delineated as follows:

(1) N represents the number of hidden states. S denotes the set of hidden states, i.e., $S = \{S_1, S_2, \cdots, S_N\}$. At time t, the state of the model is denoted by q_t, where $1 \le t \le T$, and T represents the length of the observation sequence.

(2) M represents the total number of different observation symbols. If V is the set of all observation symbols, then $V = \{v_1, v_2, v_M\}$.

(3) A represents the state transition probability distribution or the state transition matrix, where $A = a_{\mathrm{ij}}$, and $a_{ij} = P[q_t = S_i | q_{t+1} = S_j]$, for $1 \le i, j \le N$, subject to the constraints:

$$\begin{cases} 0 \le a_{\mathrm{ij}} \le 1, \\ \sum_{j=1}^{N} a_{\mathrm{ij}} = 1. \end{cases} \tag{1}$$

(4) B represents the observation probability matrix, also known as the emission matrix. $B = \{b_j(k)\}$, where $1 \le j \le N$ and $1 \le k \le M$, and $b_j(k) = P[\sigma_t = v_k | q_t = S_j]$, where σ_t is the observation symbol at time t.

(5) Π represents the initial state distribution, $\Pi = \{\pi_i\}$, where $\pi_i = P[q_1 = S_i]$, $1 \le i \le N$.

HMMs can be represented in the following three-parameter form: $\lambda = (A, B, \Pi)$. For discrete HMMs, observations are finite symbols from a finite symbol set, while for continuous HMMs, observations are described using a probability density function. The most commonly used probability density model is a mixture of Gaussian probability density functions:

$$b_j(o) = \sum_{m=1}^{M} C_{\mathrm{jm}} b_{\mathrm{jm}}(o). \tag{2}$$

In the above equation, C_{jm} represents the number of components in the mixture of Gaussian probability density functions, which is distinct from the total number of observation symbols "M" in discrete HMMs. The mixture coefficients satisfy the following condition:

$$\sum_{m=1}^{M} C_{\mathrm{jm}} = 1. \tag{3}$$

In the equation, $b_j(j)$ represents the single Gaussian probability density function for the m-th component of the j-th state.

The practical application of Hidden Markov Models (HMMs) involves addressing three key problems: (1) Given an observation sequence $O = o_1 o_2 \cdots o_r$ and the model parameters $\lambda = (A, B, \Pi)$, how to calculate $P = (O|\lambda)$, which is the probability of generating the observation sequence according to the given model. (2) Given an observation sequence $O = o_1 o_2 \cdots o_r$ and the model parameters $\lambda = (A, B, \Pi)$, how to choose the optimal state sequence = $q_1 q_2 \cdots q_n$ that best explains the observation sequence O. (3) How to adjust the model parameters λ to maximize $P = (O|\lambda)$. Problem (3) focuses on optimizing the model parameters using the observed sequence as the training data. In the majority of HMM applications, training is of utmost importance.

3. Principle of Fault Prediction Based on HMM

A predictive algorithm for common bearing faults is developed utilizing the Hidden Markov Model (HMM) [23], which encompasses the subsequent steps (as depicted in Figure 1) [5].

To commence, the HMM model is trained utilizing historical data. Vibration signal historical data are extracted for distinct bearing states, and several training sequences are derived from these datasets. The training sequences undergo vector quantization through the K-means algorithm. Subsequently, HMM models corresponding to various bearing states are trained, employing the forward-backward (F-B) algorithm. This process yields HMM model parameters that accurately represent the characteristics of each bearing state. Following this, a likelihood probability model is established.

The present measured vibration signal is input into the constructed HMM model for the purpose of ascertaining the current bearing state. Subsequently, the maximum likelihood probability of the bearing being in a specific state is computed. This likelihood probability is then used as a feature parameter to construct a time series of feature parameters, denoted as $x(n)$, with a time interval of Δt. Model identification and parameter calibration are performed, including calculating the model order and parameters. Finally, based on the established HMM model, future feature parameters are predicted for time instances t_i (where $i = 1, 2, \ldots, n$) after time t_0. The predicted feature parameters u_i are compared with the given threshold values A_1 and A_2. Bearing faults or failures are determined when $u_i > A_1$ and $u_i > A_2$, respectively. Consequently, the time intervals T_1 and T_2, as well as the corresponding time instances t_1 and t_2 ($t_{1,2} = t_0 + T_{1,2}$), when the bearing reaches the fault or failure state are obtained [5].

For obtained fault prediction results, define prediction confidence C.

$$C = \left(1 - \left|\frac{T_{i\_\text{real}} - T_i}{T_{i\_\text{real}}}\right|\right) \times 100\%, \ (i = 1, 2). \tag{4}$$

In the equation, T_i represents the predicted time for bearing failure and malfunction occurrence, while T_{i_real} denotes the actual time of bearing failure and malfunction occurrence.

4. Rolling Bearing Monitoring and Fault Diagnosis

Vibration analysis was conducted using a test rig for the rotor of an aircraft environmental control system (ECS) turbocharger rolling bearing. The test rig featured a horizontally oriented rotor structure that was driven by a motor. The primary structural components are depicted in Figure 2.

Various types of bearing faults were preconfigured, and accelerated life tests of rolling bearings were conducted under multiple operating conditions to obtain vibration test signal data. By comparing the vibration monitoring data under different operating conditions, the vibration fault characteristics were analyzed.

5. Vibration Analysis of Overheated Rolling Bearings

Experimental tests were conducted to investigate the overheating fault of rolling bearings, and the effectiveness of the fault prediction algorithm in predicting overheating faults was evaluated using the experimental data. The vibration signals of the measured overheated rolling bearings are illustrated in Figure 3.

5.1. Training HMM Model Based on Historical Data. After 200 seconds of testing, the temperature of the outer surface of the bearing housing increased from room temperature to approximately 110°C. Therefore, it is assumed that the bearing was in a normal state at 30 seconds and in an overheated fault state at 200 seconds. A 1.2-second vibration signal was extracted starting from 30 seconds as a training sequence for the HMM model, representing the normal state of the bearing. Similarly, a 1.2-second vibration signal was extracted starting from 200 seconds as a training sequence for the HMM model, representing the faulty state of the bearing.

A sampling time interval of $\mathrm{dt}_1 = 0.2$ seconds and a sampling duration of $l_1 = 0.1$ seconds were set, and each HMM model was trained using six training sequences. The model parameters, including the state transition matrix, observation probability matrix, and initial state probability vector, were obtained for both sets of HMM models.

5.2. Thresholds for Bearing Fault Feature Parameters. The six training sequences for the bearing fault states were introduced into the trained HMM models, and state recognition was performed. The maximum likelihood probabilities for each sequence belonging to the two categories of bearing states were computed, and the results are presented in Table 1.

Calculation of the average value of the probability difference in Table 1 yields 11.1713. Consequently, the threshold A_2 for determining the bearing fault state is set to 12.

5.3. State Recognition Based on Current Data. The vibration measurement data of the bearing from 30 to 200 seconds were utilized, with a sampling time interval of $\mathrm{dt}_1 = 0.2$ seconds. The maximum likelihood probabilities were computed, and the results are depicted in Figure 4.

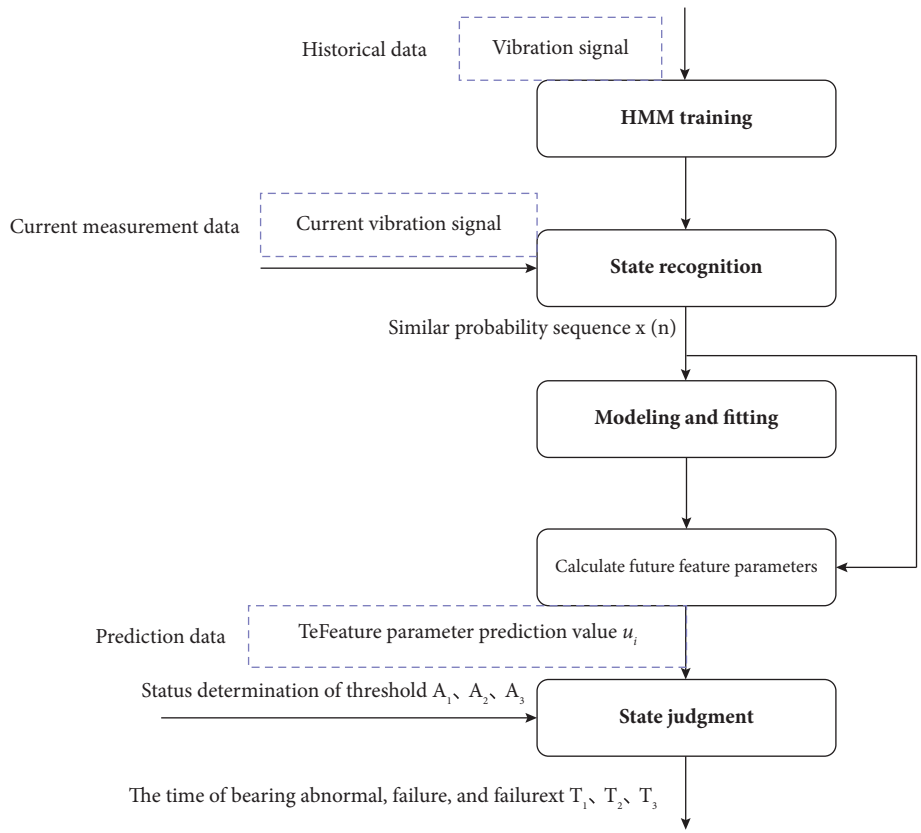

Figure 1: Schematic diagram of fault prediction based on the HMM method.

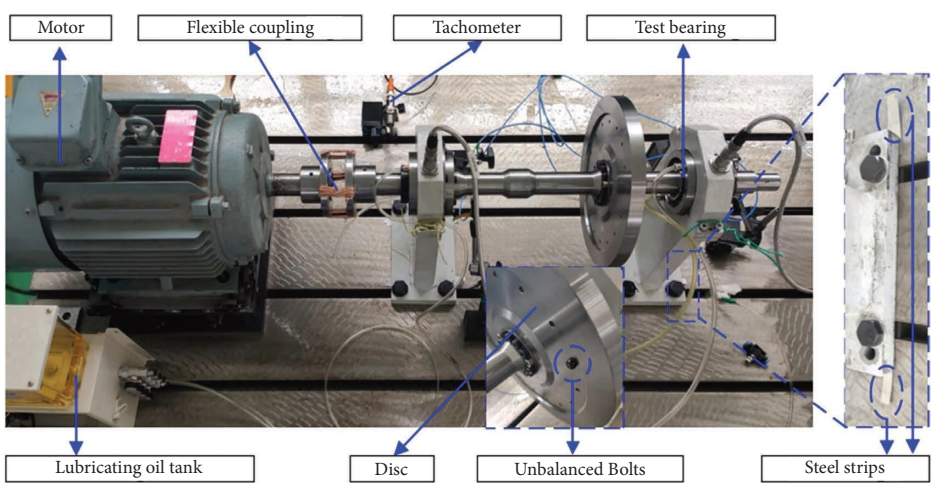

Figure 2: The rotor supported on the rolling bearings test-platform.

To provide a clearer depiction of the state variations during the temperature rise process, the average value sequence was processed. Firstly, the stages of bearing speed increase and decrease were removed to eliminate the influence of rotational speed on state evolution. Next, the absolute values of ten adjacent average values were taken, summed, and then averaged to obtain the computed result as a feature parameter. Finally, the process was repeated by shifting one average value backward, and the results are presented in Figure 5.

It can be observed that throughout the entire heating process, the likelihood probability fluctuates between 2 and 8, indicating a certain degree of error in the HMM model's recognition of bearing states before and after heating.

6. Analysis of Rolling Bearing Cage Fracture under Off-Center Load Conditions

To conduct experimental tests for bearing cage fracture faults under biased load conditions, a meticulously

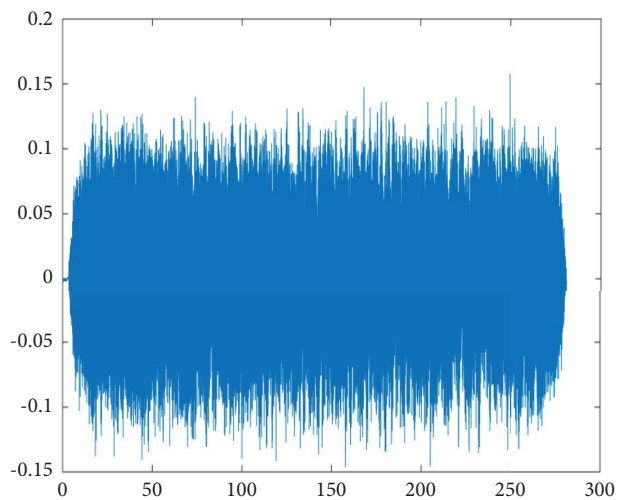

Figure 3: Vibration signals of overheating faults of the rolling bearings.

Table 1: Recognition result of temperature rising state.

Sequence	1	2	3	4	5	6
Normal status	−83.5185	−92.1298	−90.8108	−84.8107	−93.3492	−84.8745
Failure status	−75.6440	−78.4925	−76.6744	−76.7286	−76.3240	−78.6024
Difference	7.8745	13.6373	14.1364	8.0821	17.0252	6.2720

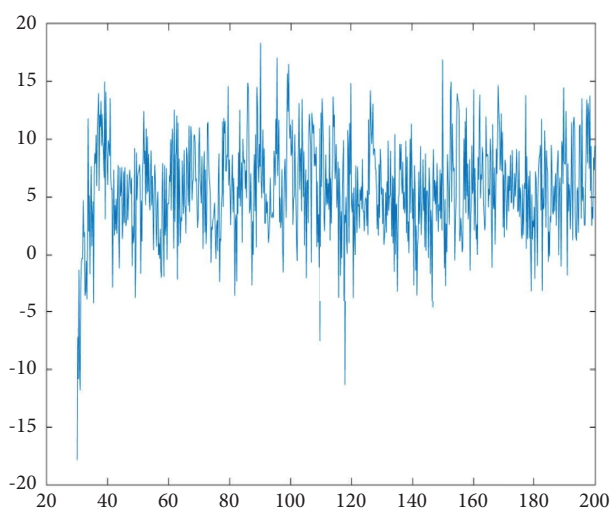

Figure 4: Likelihood probability of temperature rising state.

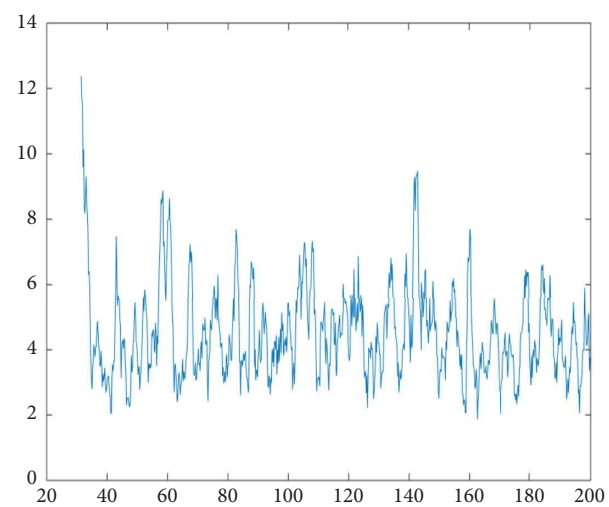

Figure 5: Arranging results of likelihood probability of temperature rising state.

designed procedure was employed. This procedure involved placing thin steel strips, each with a thickness of 0.25 millimeters, between the bearing seat and the base. A total of 8 strips were used, with 4 on each side, stacked together. The strategic placement of these steel strips induced a controlled tilt in the bearing seat along the vertical axis, resulting in a precisely regulated relative angular displacement between the inner and outer bearing rings. The relationship between the thickness of the steel strips and the width of the bearing seat is described by the following formula:

$$\theta = \arctan\left(\frac{b}{l}\right), \tag{5}$$

where b represents the thickness of the steel strips, and l signifies the width of the bearing seat.

As a result of this well-calculated arrangement, the steel strips theoretically induced a tilt of 0.4 degrees in the bearing seat, thereby theoretically imparting a 0.4-degree angular displacement between the axes of the inner and outer bearing rings. It is important to note that the actual angular displacement of the inner and outer bearing ring axes was

slightly less than the theoretically calculated value due to the influence of bearing seat cover assembly tightness and assembly clearances. During the experimental phase, the primary data sources included vibration signals and bearing seat acceleration data. After completing the experimental tests, the bearings were carefully disassembled to enable a detailed examination of surface morphology. Subsequently, the empirical data collected during the experiment were used to rigorously evaluate the performance of the fault prediction algorithm in detecting bearing cage fracture faults under biased load conditions. The vibration signals of rolling bearings afflicted by cage fracture faults under biased load conditions are illustrated in Figure 6.

6.1. Training HMM Models Based on Historical Data. The vibration signal in Figure 6 indicates that the bearing is in two completely different states at 0 s and 200 s, respectively. Therefore, 12 s of vibration signal is extracted, starting from 0 s, as the training sequence for the HMM model, representing the normal state of the bearing. Similarly, 12 s of vibration signal is extracted, starting from 200 s, as the training sequence for the HMM model, representing the faulty state of the bearing.

With a sampling time interval of 0.2 s ($dt_1 = 0.2s$), six training sequences are obtained for each HMM model. This process is repeated for both HMM models, resulting in two sets of HMM model parameters, including the state transition matrix, observation probability matrix, and initial state probability vector.

6.2. Threshold for Bearing Fault Feature Parameters. All 210 s of experimental data for the bearing is fed into the two trained HMM models for state recognition. The maximum likelihood probabilities for each sequence belonging to the two classes of bearing states are calculated, and the results are shown in Figure 7.

In order to better illustrate the changes in the state of the rolling bearing cage fracture process under biased load conditions, the average value sequence is processed. The summation and averaging of every 2 seconds (i.e., 8 probability values) are performed to obtain the computed result as the feature parameter. Subsequently, one average value is shifted backward, and the calculation is saved, as shown in Figure 8 [5].

As depicted in Figure 8, the maximum likelihood probability reaches its peak at 197.4 s, with a value of 32.61. The measured vibration of the bearing at this moment (Figure 6) indicates a highly intense vibration, highlighting clear fault features. Consequently, the threshold for determining the bearing fault state, A_2 is set to 32 [5].

6.3. Bearing Fault State Recognition Based on HMM. Using the vibration measured data from the bearing within the time range of 0 to 240 seconds, with a sampling time interval of 0.2 s ($dt_1 = 0.2$ s) and a sampling duration of $l1 = 45$ s, 200 maximum likelihood probabilities are calculated, as shown in Figure 9.

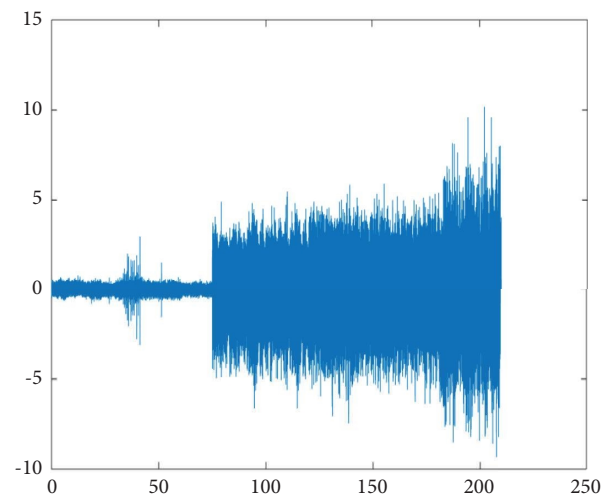

Figure 6: Vibration signals of cage fracture under partial load condition experiment of the rolling bearings.

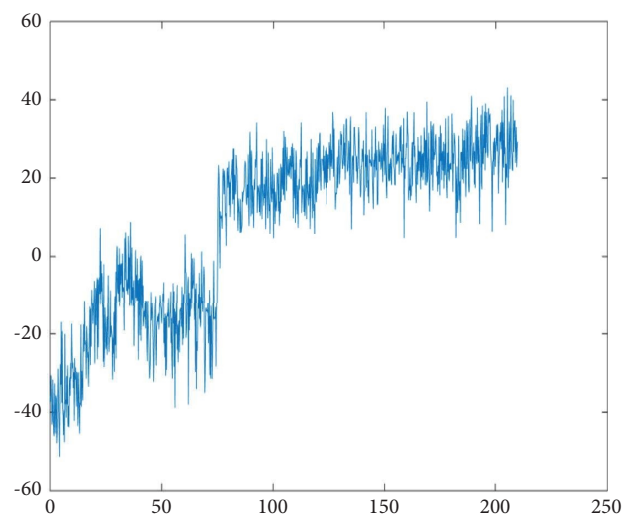

Figure 7: Likelihood probability of vibration signals of cage fracture under partial load condition [5].

Iterative calculations are performed on the feature parameters, and if the computed feature parameter exceeds the threshold A_2 for the fault state, the prediction of the time T_2 when the bearing reaches the fault state is obtained.

The comparison between the calculated results of the feature parameter predictions and the actual values is shown in Figure 10. It can be observed that there is a good fit between the predicted values of the feature parameters and the actual values, indicating that the established HMM model can accurately reflect the actual variation pattern of the feature parameters.

The prediction results are presented in Figure 10 and Table 2. The actual value of the bearing failure time t_2 is 196 s, while the predicted value is 190.4000 s. The actual value of the time T_2 to bearing failure is 157.2003 s, and the predicted value is 151.6102 s, resulting in a prediction error of 5.5901 s and a confidence level of 96.44% [5].

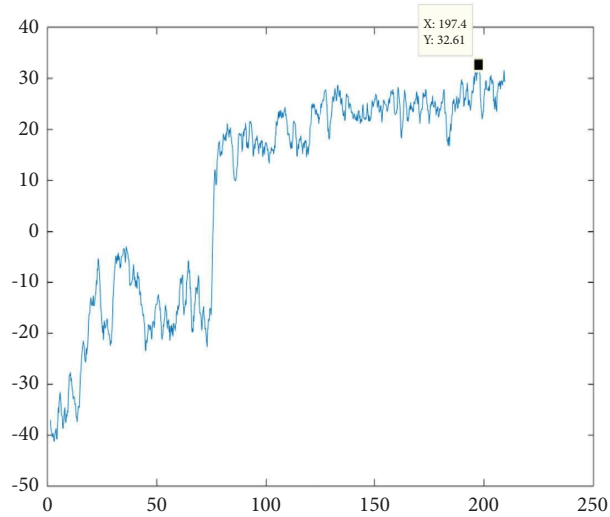

Figure 8: Averaged likelihood probability of vibration signals of cage fracture under partial load condition [5].

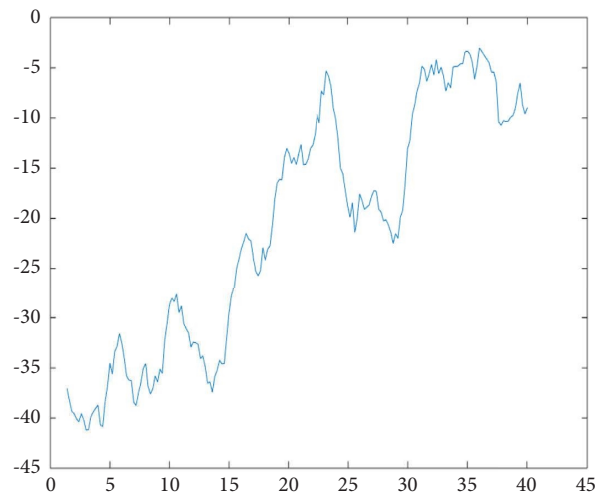

Figure 9: HMM identification results of vibration signals of cage fracture under partial load condition.

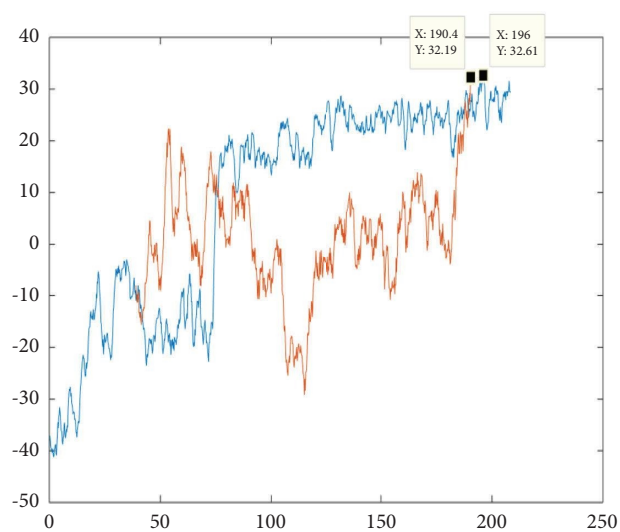

Figure 10: Forecast effect test of HMM identification results of vibration signals of cage fracture under partial load condition [5].

Table 2: Forecast result of HMM identification results of vibration signals of cage fracture under partial load condition.

	Actual value	Predictive value	Predictive error	Confidence (%)
T_2	157.2003	151.6102	5.5901	96.44

7. Conclusions

In this research, a methodology founded on the Hidden Markov Model (HMM) approach, utilizing the vibrational responses of rolling bearings was applied to detect abnormal vibrational signals in aircraft environmental control turbofan rolling bearings. The computed results of the predicted feature parameters were juxtaposed against the actual values. Acknowledging the nonstationary attributes of rolling bearing fault signals, a bearing fault diagnosis technique predicated on the HMM model was postulated. This approach leverages the HMM model to formulate precise models from deconstructed dynamic data, thereby facilitating the identification of faults such as fractured bearing cages under biased load conditions. Nevertheless, it was observed that the performance in identifying overheating faults in bearings was less than optimal.

Data Availability

The data that support the findings of this study are available from the corresponding author upon reasonable request.

Conflicts of Interest

The authors declare that there are no conflicts of interest regarding the publication of this paper.

Acknowledgments

The authors would like to acknowledge the support of the National Natural Science Foundation of China (No. 12172210).

References

[1] Z. Zhang, *Typical Fault Diagnosis of Aircraft Wheel Rolling Bearings Based on Particle Filtering*, Civil Aviation University of China, Tianjin, China, 2021.

[2] F. Wang, X. Chen, and D. Yan, "Fuzzy C-means using manifold learning and its application to rolling bearing performance degradation assessment," *Journal of Mechanical Engineering*, vol. 52, no. 15, pp. 59–65, 2016.

[3] J. Wang, G. Chen, and H. Wang, "Condition assessment for aero-engine rolling bearings based on posterior probability SVM," *Bearing*, vol. 5, no. 5, pp. 55–59, 2015.

[4] Z. Hu, J. Hu, and L. Xie, "Review on signal processing for rolling bearing vibration," *Chinese Journal of Construction Machinery*, vol. 14, no. 6, pp. 525–532, 2016.

[5] J. Yan, J. Yu, W. Zhuang, L. Li, and Y. Chen, "Study on fault feature extraction of ECS turbine bearing by combination of EEMD and HMM," *Journal of Physics: Conference Series*, vol. 2181, no. 1, Article ID 012037, 2022.

[6] W. Li, W. Shan, and X. Zeng, "Bearing fault identification based on deep belief network," *Journal of Vibration Engineering*, vol. 29, no. 2, pp. 340–348, 2016.

[7] L. Li and M. Tang, "Research on fault severity evaluation method for rolling bearing," *Bearing*, vol. 4, no. 4, pp. 33–37, 2009.

[8] J. Zhang, W. Zhan, and M. Ehsani, "On-line fault diagnosis of electric machine based on the Hidden Markov Model," in *Proceedings of the IEEE Transportation Electrification Conference & Expo*, pp. 1–7, Dearborn, MI, USA, June 2016.

[9] X. Jiang, S. Li, and C. Cheng, "A novel method for adaptive multiresonance bands detection based on VMD and using MTEO to enhance rolling element bearing fault diagnosis," *Shock and Vibration*, vol. 2016, Article ID 8361289, 20 pages, 2016.

[10] Q. Lu, X. Shen, X. Wang, M. Li, J. Li, and M. Zhang, "Fault diagnosis of rolling bearing based on improved VMD and KNN," *Mathematical Problems in Engineering*, vol. 2021, Article ID 2530315, 11 pages, 2021.

[11] S. Ning, Y. Wang, W. Cai et al., "Research on intelligent fault diagnosis of rolling bearing based on improved ShufflenetV2-LSTM," *Journal of Sensors*, vol. 2022, Article ID 8522206, 13 pages, 2022.

[12] M. Mao, C. Zhou, J. Yang, B. Fang, F. Liu, and X. Liu, "Research on fault diagnosis method of rolling bearing based on feature optimization and self-adaptive SVM," *Mathematical Problems in Engineering*, vol. 2022, Article ID 6711019, 20 pages, 2022.

[13] X. He and J. Ma, "Weak fault diagnosis of rolling bearing based on FRFT and DBN," *Systems Science and Control Engineering*, vol. 8, no. 1, pp. 57–66, 2020.

[14] C. Yang, Z. Qiao, R. Zhu, X. Xu, Z. Lai, and S. Zhou, "An intelligent fault diagnosis method enhanced by noise injection for machinery," *IEEE Transactions on Instrumentation and Measurement*, vol. 72, pp. 1–11, 2023.

[15] A. Soualhi, G. Clerc, H. Razik, M. El badaoui, and F. Guillet, "Hidden Markov models for the prediction of impending faults," *IEEE Transactions on Industrial Electronics*, vol. 63, no. 5, pp. 3271–3281, 2016.

[16] T. Yu, T. Chen, and Y. Chen, "Fault diagnosis of bearing failure using HMMS," *Journal of Harbin Institute of Technology*, vol. 48, no. 2, pp. 184–189, 2016.

[17] A. Soulhi, G. Clerc, and H. Razik, "Fault prognosis based on hidden Markov models," in *Proceedings of the IEEE Workshop on Electrical Machines Design*, pp. 271–278, Control and Diagnosis, Torino Italy, March 2015.

[18] C. Feng, Q. Ding, and Z. Wu, "Study on Hidden Markov Models for faults diagnosis of rotor machine in the whole run-up process," *Journal of Zhejiang University*, vol. 36, no. 6, pp. 44–47, 2002.

[19] Q. Ding, Z. Li, and Z. Wu, "Research on fault diagnosis methods for rotating machines based on factorial Hidden Markov Model," *Power Engineering*, vol. 23, no. 4, pp. 2560–2563, 2003.

[20] J. Zhang, W. Zhan, and M. Ehsani, "On-line fault diagnosis of electric machine based on the Hidden Markov Model," in *Proceedings of the 2016 IEEE Transportation Electrification*

Conference and Expo (ITEC), pp. 1–7, Dearborn, MI, USA, June 2016.

[21] A. Soualhi, G. Clerc, H. Razik, M. El badaoui, and F. Guillet, "Hidden Markov models for the prediction of impending faults," *IEEE Transactions on Industrial Electronics*, vol. 63, no. 5, pp. 3271–3281, 2016.

[22] Y. Li, *Wear Condition Fault Recognition and Diagnosis of Rolling Bearings*, Shenyang University of Chemical Technology, Shenyang, China, 2019.

[23] B. Fang, *Research on Health State Assessment Method of Rolling Bearings*, Harbin Institute of Technology, Heilongjiang, China, 2020.